
Article:
Wang, X., Chauvat, M.P., Ruterana, P. et al. (2017) Effective absorption correction for energy dispersive X-ray mapping in a scanning transmission electron microscope: analyzing the local indium distribution in rough samples of InGaN alloy layers. Journal of Microscopy, 268 (3). pp. 248-253. ISSN: 0022-2720

https://doi.org/10.1111/jmi.102643

Effective absorption correction for energy dispersive X-ray mapping in a scanning transmission electron microscope: analyzing the local indium distribution in rough samples of InGaN alloy layers

X. Wang[1], M.-P. Chauvat[2], P. Ruterana[2] and T. Walther[1*]

[1] Department of Electronic and Electrical Engineering, University of Sheffield, North Campus, George Porter Building, Sheffield S3 7HQ, UK

[2] CIMAP, UMR 6252, CNRS-ENSICAEN-CEA-UCBN, 14050 Caen, cedex, France

*Email: t.walther@sheffield.ac.uk

Abstract

We have applied our previous method of self-consistent k*-factors for absorption correction in energy-dispersive X-ray spectroscopy to quantify the indium content in X-ray maps of thick compound InGaN layers. The method allows us to quantify the indium concentration without measuring the sample thickness, density or beam current, and works even if there is a drastic local thickness change due to sample roughness or preferential thinning. The method is shown to select, point-by-point in a two-dimensional spectrum image or map, the k*-factor from the local Ga K/L intensity ratio that is most appropriate for the corresponding sample geometry, demonstrating it is not the sample thickness measured along the electron beam direction but the optical path length the X-rays have to travel through the sample that is relevant for the absorption correction.

Introduction

Elemental maps show the spatial distribution of chemical elements in an unknown sample. Elemental mapping in a transmission electron microscope (TEM) can be performed by energy dispersive X-ray spectroscopy (EDXS) (Watanabe et al. 1997), electron energy-loss spectroscopy (EELS) (Colliex et al. 1994) or even wavelength dispersive spectroscopy (WDS) although the latter is better and more commonly applied to bulk samples in a scanning electron microscope (SEM) (Duncumb 1979). If spectra are recorded and evaluated at each pixel net intensity maps of the distribution of chemical elements can thus be obtained after background subtraction. The spectral intensity is strongly related to the number and type of atoms excited and thus to the

specimen thickness in a TEM, and for EDXS it also depends on collection solid angle, take-off angle and detector window type and thickness (Williams & Carter 1996). For a fixed set-up of EDXS detector type and position with respect to the electron beam direction, only the geometry of the sample and the beam current influence the intensity of the spectra. If the TEM specimen is not perfect flat, absorption corrections such as ZAF (Goldstein & Williams 1981; Tixier, Thomas & Bourgeot 1981), which is a standard absorption correction multiplying the specimen thickness by the cosec function of the take-off angle, will become invalid. Unfortunately, a precise measurement of the X-ray optical path length in a rough sample is almost impossible, however, the influence of the sample topography on the Ga K/L ratio can be directly measured in gallium containing specimens such as InGaN. Therefore, it is possible for a routine to automatically select a suitable *k*-factor based on the Ga K/L ratio measured in the same spectrum to interpolate the relative absorption of the indium L-line and so to quantify the chemistry of a rough InGaN sample at each point without the need for a specimen geometry measurement. We have termed such absorption correction factors, if plotted vs. measured K/L ratios, *k**-factors (Qiu et al. 2013; Walther & Wang 2015). It is worth pointing out that the *k**-factor method does also not need the electron beam current to be measured, in contrast to the zeta-factor method, which recovers the mass-thickness product indirectly from this by iteration (Watanabe, Horita and Nemoto 1996).

Experimental techniques

In this paper, a 200kV JEOL 2010F equipped with a Schottky field-emission gun (FEG) is used for exciting X-rays from an InGaN thin film specimen. Elemental mapping was carried out using an Oxford Instruments Si:Li detector with ultrathin window at nominal 25° take-off angle (Parri, Qiu and Walther 2015). The energy resolution of the EDXS system varies from 60eV (FWHM of strobe) to 136eV (FWHM of Mn K_α peak at 5895eV). 8 bit 128×100 pixels maps with a sampling of 4.72nm per pixel have been obtained by using the Oxford Instruments ISIS 300 software and a 70 micrometer condenser aperture in STEM mode, yielding ~16.6mrad semi-angle of convergence and a probe ~1nm in diameter. Later, relative thickness maps were recorded from the same region using energy filtered transmission electron microscopy (EFTEM) in a JEOL R005 Z3100 microscope operated at 300kV and equipped with cold FEG, a Gatan Tridiem ER865 imaging energy filter and an Ultrascan2k charge-coupled device (CCD) camera. A 5mm entrance aperture with a 24.9 mrad collection semi-angle from a 120µm objective aperture was used to record EFTEM images from which relative thickness maps were calculated.

The sample is an $In_xGa_{1-x}N$ (nominal x=0.62) thin film cross-sectional specimen that we have previously analysed by X-ray and plasmon spectroscopy (Wang et al. 2015), which gave an average indium content of x=0.68. The sample was grown in a shower head AIXTRON reactor using triethyl-gallium (TEGa), trimethyl-indium (TMIn) for the metals and NH_3 for nitrogen, on a (0001) sapphire substrate. Due to the high In content, the 80-100nm thick InGaN film was under high compressive strain and

formed islands ~100 nm high and 200-300nm in length. The TEM specimen was prepared by conventional grinding and dimpling, followed by argon ion milling. A Gatan PIPS ion milling system was operated at 5keV down to 0.6keV ion energy for final polishing, to minimize the ion beam damage to the specimen.

Applying absorption corrected method to EDXS element mapping

The self-consistent X-ray absorption correction method employing k*-factors, as defined (Walther & Wang 2015) and tested for individual spectra (Walther & Wang 2016) in our previous InGaN work was applied to calculate the indium content for each pixel of the X-ray elemental map. In_L, Ga_K and Ga_L maps and several maps for background correction were recorded to construct background subtracted intensity maps of I_{InL}, I_{GaK} and I_{GaL}. The choice of nominal background follows the 'Fiori' definition (Fiori et al. 1976), where the background map was recorded for a nominal element that the specimen did not contain but whose X-ray lines were close to that of the element of interest. Then linear extrapolation (or interpolation, if performed for several lines on both sides of the real lines) could be used to subtract an approximate background map. The background maps (not shown as dominated by shot noise of a few counts) and the Ga K/L maps shown in Figure 4 were subsequently smoothed by a 3×3 pixels low pass filter to reduce noise before further processing. Then maps of the k*-factors for In_L with respect to Ga_K and In_L with respect to Ga_L were generated by using the smoothed Ga K/L map and comparison to Monte Carlo simulations (Parri, Qiu & Walther 2015; Walther & Wang 2016). Since the k*-factors change exponentially as a function of Ga K/L ratio, which in thin regions where the count rates are low can be very noisy, we confined the Ga K/L ratio to the physically meaningful range of 0.5-6 by thresholding. The background subtraction was fine tuned to fractional counts (the Oxford ISIS software only works with integer count numbers) in the pure GaN area, by subtracting a fraction of the smoothed nominal background (of the order of a few counts for Ga_L and fractions of a single count for all other lines) so that the resulting x map histograms could be fitted by Gaussian distribution functions centered at zero (cf Figure 5). It is noted that this was only necessary as our vintage acquisition software cannot store whole spectral data sets, which is possible in modern systems and then allows a much more reliable background fit for each X-ray line at each point when generating maps. Then, we have applied the k*-factor correction to every point in the In_L, Ga_K and Ga_L maps, and thus obtained indium concentration maps using Ga_K or Ga_L lines for quantification.

Experiment result and discussion

Figure 1a) is an annular dark field image where regions thicker or richer in indium appear brighter. The light grey material at the bottom left is the GaN buffer, on which an ~80nm thick InGaN is visible as a bright stripe, on top of which two facetted InGaN islands are located that appear to have been cut through and so are thinner in transmission, as can be seen from the relative thickness map in Figure 1b). It is clear

that the film below one island is much thinner at its base. Such trough-like structures have frequently been observed in this sample (Walther et al. 2017).

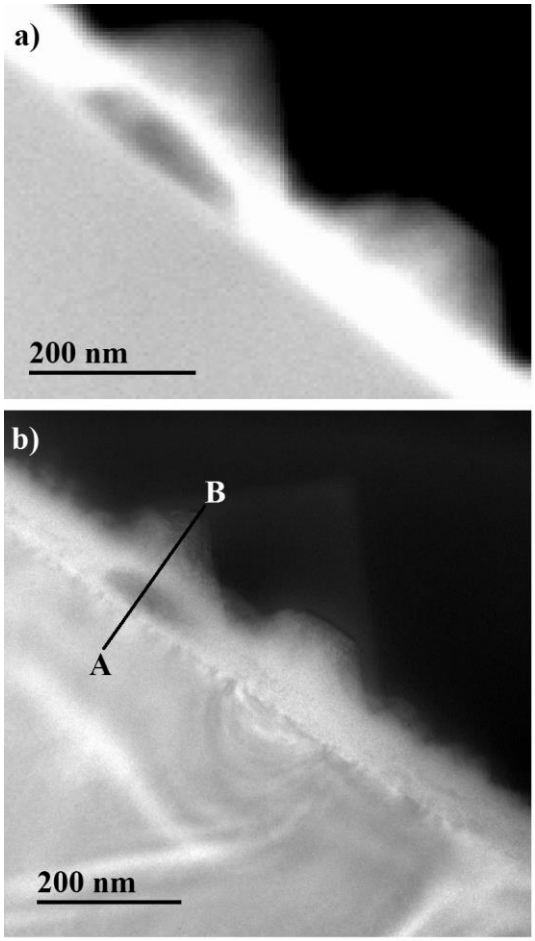

Figure 1: a) ADF image and b) relative thickness map (E_0=300kV, β=25mrad, min=0.30, max=3.73, where t/λ=1.0 in the faintly visible square of carbon contamination) from EFTEM, with position for line profile in Figure 2 as indicated.

A relative thickness map was recorded by EFTEM to measure the thickness of the same area. In Figure 1b), the region underneath the larger island clearly has a high degree of local thickness change. The absolute thickness of the sample has then been calculated by multiplying the relative thickness (t/λ) map from Fig. 1b) by the value of the inelastic mean free path, λ , under the approximation

$$\lambda = \frac{106\mathrm{F}\ E_0/E_\mathrm{m}}{\ln(2\beta E_0/E_\mathrm{m})} \qquad (1)$$

where E_0 is incident electron energy in keV, β is the collection angle in mrad, F is a relativistic factor and E_m is the average energy loss in eV which, for a material of average atomic number Z, is approximately given by $7.6Z^{0.36}$ (Egerton 1996). Z for ternary $In_xGa_{1-x}N$ alloy can be expressed as

$$Z_{\mathrm{InGaN}} = \frac{(1-\mathrm{x})\ 31^{1.3}+\mathrm{x}\ \ 49^{1.3}+2\times7^{1.3}}{(1-\mathrm{x})\ 31^{0.3}+\mathrm{x}\ 49^{0.3}+2\times7^{0.3}} \qquad (2)$$

A line profile along line AB in Figure 1b, converted into absolute thickness values

using above equations (λ = 99nm for InGaN) after subtraction of the relative thickness of the carbon film, is shown in Figure 2. Assuming the thickness drops gradually from 225nm in the GaN buffer layer to around 100nm in the InGaN thin film area underneath, the average depth of the depression near the interface is ~120nm. The width of this preferentially thinned area along the growth direction is 44nm. X-ray photons generated near the bottom of this thinned region therefore cannot reach the detector without having to travel through the InGaN because of the steep angle of the sidewalls of the depression being much larger than the take-off angle of the X-ray detector, regardless of which surface the roughness is confined to.

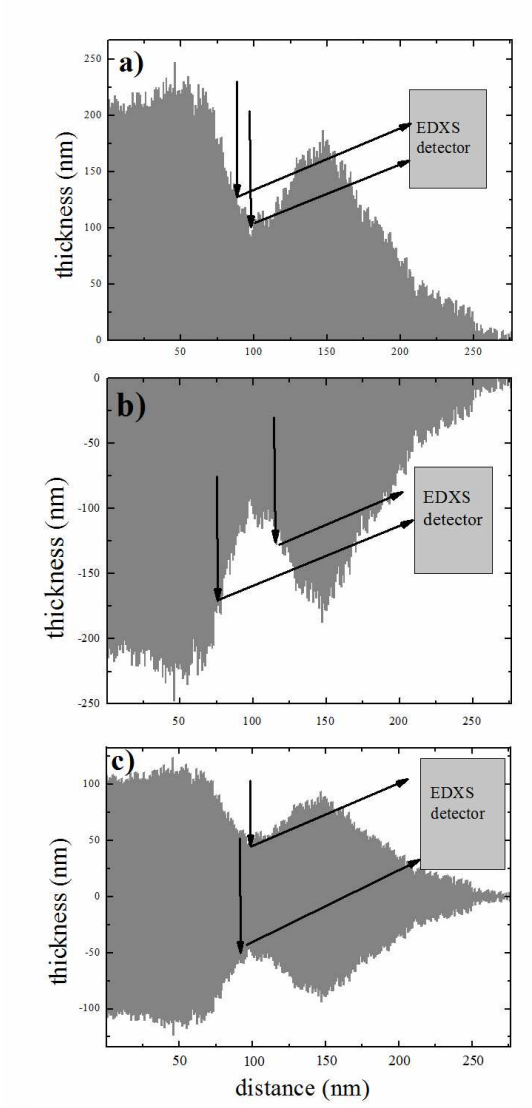

Figure 2: X-ray path sketches for a) case of top surface roughness only; b) bottom surface roughness only; c) symmetrical surface roughness on top and bottom surfaces.

In our system the EDXS detector has a take-off angle around 25° if the specimen is flat and not tilted (Parri, Qiu & Walther 2015). The generated X-ray photons must therefore pass through the InGaN material before they reach the detector. From the

specimen thickness map in Figure 1b) and the inelastic mean free paths we have constructed several possible cross-sectional thickness profiles, which are sketched in Figure 2, assuming the roughness is either confined to the top surface (Fig. 2a), the bottom surface (Fig. 2b) or identical on both surfaces (Fig. 2c). Even if the dip in specimen thickness is only half of the ~120nm estimated above, in the most optimistic case of a symmetric arrangement, as sketched in Fig. 2c), then a significant absorption correction will still be necessary despite the locally reduced thickness. This would still be true and the geometry change only marginal if we had tilted the specimen by the maximum tilt angle of 25° our ultra-high resolution pole-piece permits towards the X-ray detector – here such a tilt was not applied to demonstrate that our quantification method can cope well with rather extreme examples of absorption correction.

X-ray maps were then recorded from the same region as the one in Figure 1 for In_L, Ga_K, Ga_L and N_K, shown in Figure 3.

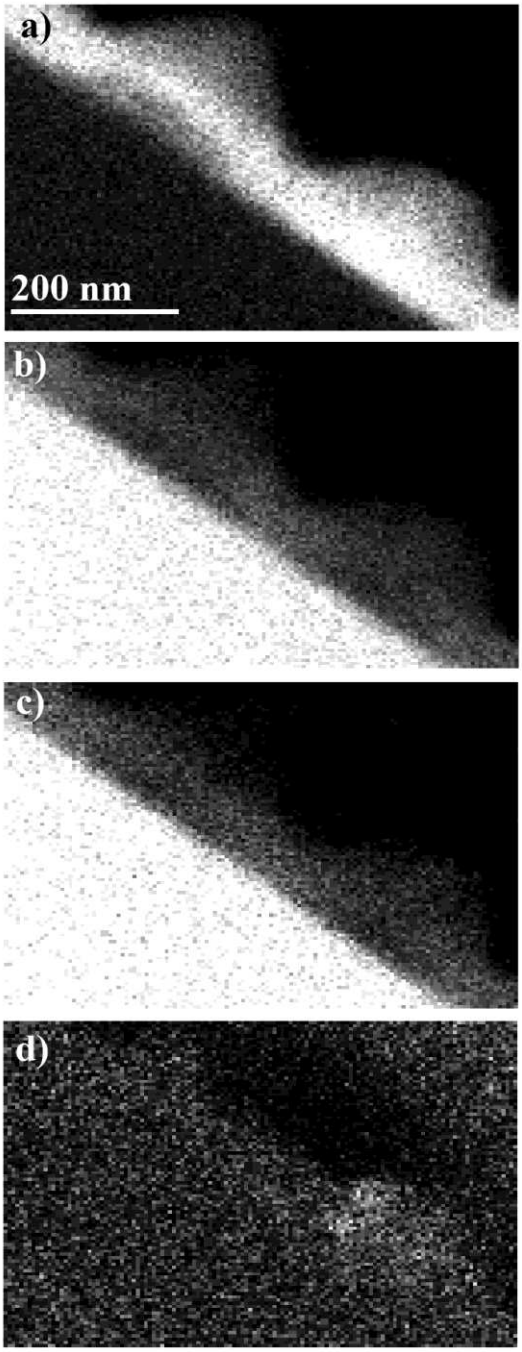

Figure 3: Elemental maps after background subtraction for a) In_L (In_L^{max}=60 counts); b) Ga_K (Ga_K^{max}=70 counts); c) Ga_L (Ga_L^{max}=40 counts); d) N_K (N_K^{max}=11 counts).

Since EDXS with a window in front of the Si:Li detector is not very sensitive to light elements (Williams & Carter 1996), the N_K map in Fig. 3d) is very noisy and cannot be quantified. Applying the self-consistent absorption correction on the basis of the Ga K/L ratio map, maps of the distribution of k^* and x values from both Ga K and L lines are presented in Figure 4.

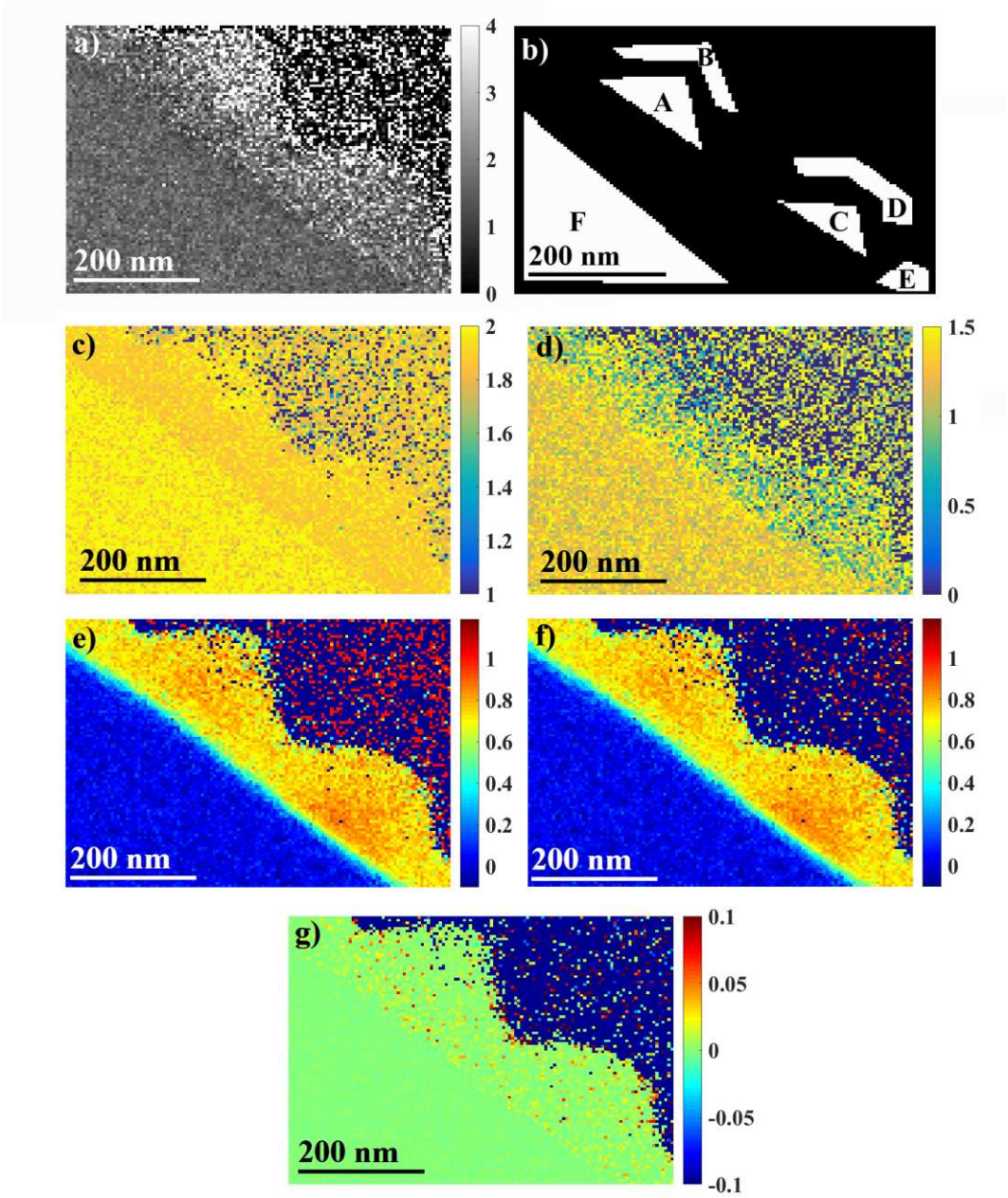

Figure 4: a) Ga K/L ratio map; b) definition of regions masked for histogram analysis; c) map of $k^*_{InL,GaK}$; d) map of $k^*_{InL,GaL}$; e) x map calculated from Ga_K; f) x map calculated from Ga_L; g)=e)–f) difference map Δx from Ga_K and Ga_L lines.

Figures 4c) and 4d) demonstrate a rather homogenous k^* value distribution in the InGaN film where the preferentially thinned region at the bottom of the large facetted island visible in Figure 1 is no longer observed. Figures 4 e) and 4f) show maps of the indium content x calculated from Ga_K and Ga_L lines and the corresponding absorption factors from 4c) and 4d), both demonstrating that the preferentially thinned area in Figure 1 consists of InGaN of chemical composition similar to the flat layer region (for minor differences see Table 1 and discussion thereof) and is neither a hole in the specimen filled with glue nor some thinner GaAs as could have been guessed from imaging studies alone. The difference map of indium concentrations in Figure 4 g) has

a mean value of near zero with a standard deviation of ±0.036, which shows the consistency of the results from quantification of Ga_K and Ga_L within noise levels.
The histograms of x values calculated for the GaN buffer from both Ga_K and Ga_L lines are depicted in Figure 5. Performing fits with Gaussian functions, the fitted curves both peak at x_{GaN}=0.011-0.013 and have FWHM values of 0.10, which agrees with a ±0.04 standard deviation (rms). In concentration maps from InGaN alloys are expected to have slightly larger statistical spreads, due to random alloy fluctuations and the possibility of alloy de-mixing and/or segregation. Histograms of the x_{In} distribution from five areas of InGaN are shown in the lower rows of Figure 5 for comparison, where the regions are described by the masks defined in Figure 4b).

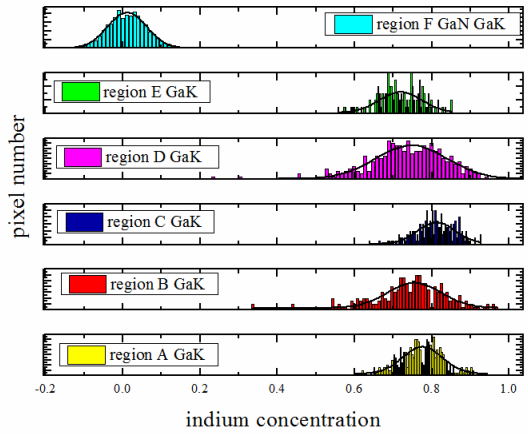

Figure 5: x map histograms of regions A-F defined in Figure 4b), as calculated from Ga_K (similar ones from Ga_L are almost identical and not shown).

The histograms of indium concentrations in the areas A-F have again been fitted by Gaussian functions, and the fitting parameters and results are listed in Table 1.

region	peak for Ga_K	peak for Ga_L	standard deviation of Ga_K	standard deviation of Ga_L
A	0.793	0.786	0.055	0.051
B	0.751	0.745	0.093	0.093
C	0.810	0.812	0.047	0.051
D	0.740	0.736	0.072	0.072
E	0.717	0.719	0.055	0.055
F	0.011	0.013	0.036	0.036

Table 1: fitting parameters for all regions A-F defined in Figure 4b)

As depicted in Table 1, consistent indium concentrations can be obtained from quantification of Ga_K and Ga_L maps. A higher indium concentration of x≈0.8 is observed in regions A & C, at the base of the islands near the InGaN/GaN interface, confirming segregation of indium as observed by EELS (Walther et al. 2017). Regions B, D & E have slightly lower indium concentrations of x≈0.7, also in agreement with our previous EELS analysis. The result proves that the indium concentration can be

determined reliably from EDXS, independent of the sample thickness.

Conclusion

We have successfully applied our self-consistent absorption correction method to quantify the indium concentration in compositional maps of a rough InGaN sample. The *k**-factor selection is not based on the sample thickness along the electron beam direction but on the measured Ga K/L intensity ratio and thus the X-ray optical path length to the detector. The resulting indium concentration maps confirm a slighhtly higher indium content underneath larger island structures.

References

Colliex, C., Tencé, M., Lefèvre, E., Mory, C., Gu, H., Bouchet, D. and Jeanguillaume, C. (1994) Electron energy loss spectrometry mapping. *Mikrochim. Acta* **114**(1), 71-87.

Duncumb, P (1979) X-ray microanalysis. *J. Microsc.* **117**(1), 165-174.

Egerton, R.F. (1996) *Electron Energy-Loss Spectroscopy in the Electron Microscope*. Plenum Press, New York, 2nd edition, p. 305.

Fiori, C.E., Myklebust, R.L. and Heinrich, K.F.J. (1976) Prediction of Continuum Intensity in Energy-Dispersive X-ray Microanalysis. *Anal. Chem.* **48**(1), 172-176.

Goldstein, J.I. and Williams, D.B. (1981) X-ray microanalysis of thin specimens. In: *Proc. Quantitative Microanalysis with High Spatial Resolution*, The Metals Society, London, UK. pp. 5-14.

Parri, M.C., Qiu, Y. and Walther, T. (2015) New pathways for improved quantification of energy-dispersive X-ray spectra of elements with multiple X-ray lines rom thin foils investigated in transmission electron microscopy. *J. Microsc*. **260**(3), 427-441.

Qiu, Y., Nguyen, V.H., Dobbie, A., Myronov, M. and Walther, T. (2013) Calibration of thickness-dependent k-factors for germanium X-ray lines to improve energy-dispersive X-ray spectroscopy of SiGe layers in analytical transmission electron microscopy. Proc. 18th Microsc. Semicond. Mater. Conf., Oxford, UK. *J. Phys. Conf. Ser.* **471**, 012031.

Tixier, R., Thomas, B. and Bourgeot, J. (1981) Principles, limits and statistical evaluation of quantitative X-ray analysis. In: *Proc. Quantitative Microanalysis with High Spatial Resolution*, The Metals Society, London, UK. pp. 15-22:

Walther, T. and Wang X. (2015) Self-consistent absorption correction for quantitative energy-dispersive X-ray spectroscopy of InGaN layers in analytical electron spectroscopy. Proc. EMAG-2015. Manchester, UK. *J. Phys. Conf. Ser.* **644**, 012006.

Walther, T. and Wang, X. (2016) Self-consistent method for quantifying indium content from X-ray spectra of thick compound semiconductor specimens in a transmission electron microscope. *J. Microsc.***262**(2):151-156.

Walther, T., Wang, X., Angadi, V.C., Ruterana, P., Longo, P. and Aoki, T. (2017) Study of phase separation in an InGaN alloy by electron energy loss spectroscopy in an aberration corrected monochromated scanning transmission electron microscope. *J. Mater. Res.* **32**(5), 983-995.

Wang, X., Chauvat, M.-P., Ruterana, P. and Walther, T (2015) Combination of electron energy-loss spectroscopy and energy-dispersive X-ray spectroscopy to determine indium concentration in InGaN thin film structures. *Semicond. Sci. Technol.* **30**(11), 114011.

Wang, X., Chauvat, M.P., Ruterana, P. and Walther, T. (2016) Investigation of phase separation in InGaN alloys by plasmon loss spectroscopy in TEM. *MRS Advances* **1**(40), 2749-2756.

Watanabe, M., Carpenter, D.T., Barmak, K. and Williams, D.B. (1997) Quantitative X-ray mapping with high resolution. Proc. EMAG97, Cambridge, UK. *Inst. Phys. Conf. Ser.* **153**, 295-298.

Watanabe, M., Horita, Z. and Nemoto, M. (1996) Absorption correction and thickness determination using the zeta factor in quantitative X-ray microanalysis. *Ultramicroscopy* **65**(3-4), 187-198.

Williams, D.B. and Carter, C.B. (1996) *Transmission Electron Microscopy-Spectrometry IV*. Springer, New York, p. 561.